ADAPTIVE BOUNDARY CONTROL VIBRATION SUPPRESSION OF FLEXIBLE MANIPULATOR BASED ON IMPROVED RBF NEURAL NETWORK

Qingchun ZHENG[1,2], Zhiyong WEI[1,2,3], Peihao ZHU[1,2*], Wenpeng MA[1,2], Jieyong DENG[4]

With lighter weight, lower power consumption, and higher flexibility, flexible manipulators have been widely used in industrial fields. However, it is easy to produce elastic deformation, resulting in vibration. In this paper, an improved radial basis function (RBF) neural network (NN) for adaptive boundary control is proposed. The partial differential equation (PDE) model of the flexible manipulator is established, and the asymptotic stability of the system is proved by the first Lyapunov method. Finally, simulation results show that the proposed control method can eliminate the low-amplitude angular fluctuation and the high-amplitude angular velocity fluctuation.

Keywords: adaptive control, RBF neural network, flexible manipulator, PDE model, vibration suppression

1. Introduction

With the development of industrial production, industrial manipulators have been widely used in various fields of industrial production. Due to its smaller size, lighter structure, and lower power consumption, flexible manipulators have been widely used in industrial production, aerospace, search and rescue. However, the rigidity of flexible manipulator is worse, which makes flexible manipulators generate vibration. Therefore, how to suppress the vibration of flexible manipulator has gradually become one of the hot issues.

The vibration suppression of manipulator is mainly divided into two directions: passive suppression and active suppression. Passive suppression is to suppress the vibration of manipulators by changing original structures. However, due to long development cycle time and high development cost, it has been gradually abandoned. The active suppression is realized by control algorithms to

[1] Tianjin Key Laboratory for Advanced Mechatronic System Design and Intelligent Control, Tianjin University of Technology, Tianjin, 300384, China.
[2] National Demonstration Center for Experimental Mechanical and Electrical Engineering Education (Tianjin University of Technology).
[3] School of Mechanical Engineering, Tianjin University of Technology, Tianjin, 300384, China.
[4] Jiangxi Technical College of Manufacturing, Nanchang Jiangxi 330095, China.
* E-mail: zhupeihao_gp@163.com

suppress the vibration of manipulators. With the development of control theory, active control based on control algorithms has become one of the mainstream methods.

At first, the vibration suppression of manipulators only uses a simple control method. Kim et al. [1] took advantage of the dependence of elastic deflection and suppressed the vibration of flexible manipulators by controlling contact force. As more control algorithms are proposed, some control algorithms are applied to the vibration suppression of flexible manipulators. Mohamed et al. [2] developed a proportional integral differential (PID) controller a feedforward controller to control the vibration of manipulators. Chu et al. [3] propose a global terminal sliding mode control method for vibration suppression of a manipulator.

In recent years, the hybrid control algorithm composed of neural networks and classical control algorithms have become the mainstream vibration suppression method. Because the intelligent control algorithm has good error compensation ability, it greatly improves the vibration suppression effect and has been widely used in vibration suppression of flexible manipulators.

Shaheed et al. [4] first proposed the application of neural networks to vibration suppression of flexible manipulators. Liu et al. [5] designed an adaptive fault-tolerant control scheme, and to compensate boundary disturbance by using RBF neural network. He et al. [6] proposed a combined control algorithm suppress vibration-prone link and used an RBF neural network to compensate parameter uncertainty. Based on RBF neural network, He et al. [7] proposed a reinforcement learning control strategy for flexible manipulators to realize vibration suppression. Liu et al. [8] adopted an optimization controller based on backpropagation neural network (BPNN), which can quickly effectively suppress vibration. Zhao et al. [9] proposed a new control method composed of artificial neural network, proportional integral (PD) controller and suppress link vibration. Jia et al. [10] used singular perturbation method to decouple dynamic model into two reduced price subsystems and used neural network to approximate unknown nonlinear function. He et al. [11] integrated a new neural network adaptive law to improve learning rate of the neural network and effectively suppress vibration.

According to previous research, the hybrid control algorithm composed of intelligent control and traditional control has become the mainstream research direction. Neural networks have been widely used in compensating unknown disturbances or parameters, suppressing vibration and so on. Based on this, the main innovations of this paper are as follows:

(1) An improved RBF neural network is proposed to compensate the unknown parameter boundary compensation of a planar flexible manipulator.

(2) A boundary adaptive control method is improved to suppress the vibration of the flexible manipulator.

(3) The controller was redesigned, and a simulation platform was built to observe the vibration suppression effect of the flexible manipulator through the angle tracking and angular velocity tracking of the manipulator and the motor.

2. Dynamic modeling

In this paper, the system studied is considered as a single-link flexible manipulator in a plane. A schematic diagram of the system is shown in Figure 1. XOY is the world coordinate system, and xoy is the fixed coordinate system of the single-link flexible manipulator. The basic parameters for defining a flexible manipulator are as follows:

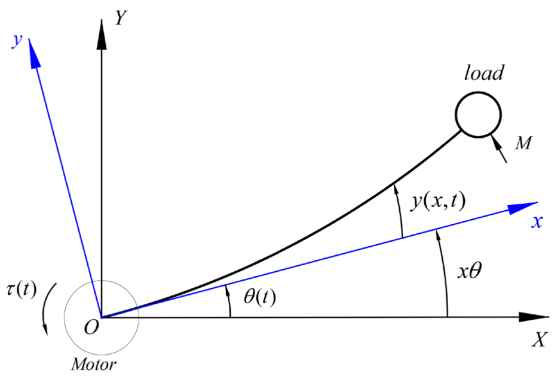

Fig. 1. Structure diagram of the flexible manipulator

Table 1

The unit of state quantity for a flexible manipulator

Symbol	Physical significance	Unit
l	The length of flexible manipulator	m
EI	The bending stiffness	N·m^2
m	The mass of system	kg
I	The moment of inertia of flexible manipulator	kg·m^2
τ	The input torque of initial terminal motor	N·m
M	The motor input control torque of end load	N·m

$\theta(t)$ is the rotation angle of the joint of flexible manipulator, ρ is the mass per unit length of manipulator, $y(x,t)$ is the elastic deformation of manipulator at point x, $x\theta(t)$ means that when point x on fixed coordinate system of flexible manipulator is rotated at θ, the fixed coordinate system of flexible manipulator is rotated relative to world coordinate system.

Any point $[x, y(x,t)]$ of the fixed coordinate system xoy on the flexible manipulator can be expressed in the inertial world coordinate system as:

$$z(x,t) = x\theta(t) + y(x,t) \tag{1}$$

Where $z(x,t)$ represents the offset of the flexible manipulator at time t. Equation(1) is just valid for small angles. Generally, the vibration of the mechanical arm is small deformation, and the conditions are valid.

When the initial position is 0, for any time t there is:

$$\begin{aligned} z(0,t) &= 0 \\ z'(0,t) &= \theta \end{aligned} \tag{2}$$

Where $z(0,t) = 0$ represents when the initial displacement is 0, the offset is 0 at time t. $z'(0,t) = \theta$ represents when the initial displacement is 0, The offset angular velocity is θ.

To establish the whole dynamic model, Hamilton principle [12,13] is applied in this paper, At time t_1 to t_2 $(t_1 < t_2)$:

$$\int_{t_1}^{t_2} (\delta T - \delta U + \delta W_{nc}) dt = 0 \tag{3}$$

Where, T is the kinetic energy of the whole flexible manipulator system, U is the potential energy of the whole flexible manipulator system, and W_{nc} is the work done by non-conservative force of flexible manipulator system.

In this equation, the kinetic energy of the whole flexible manipulator system is $T = \frac{1}{2} I\dot{\theta}^2(t) + \frac{1}{2}\int_0^L \rho \dot{y}^2(x,t)dx + \frac{1}{2} m\dot{y}^2(L,t)$, the potential energy of the whole flexible manipulator is $U = \frac{1}{2}\int_0^L EIy''^2(x,t)dx$, the work done by non-conservative force of flexible manipulator system is $W_{nc} = \tau(t)\theta(t) + My(L,t)$.

Bring all initial conditions into equation (3):

$$\begin{aligned} \int_{t_1}^{t_2} (\delta T - \delta U + \delta W_{nc}) dt &= -\int_{t_1}^{t_2}\int_0^l A\delta z(x)dxdt - \int_{t_1}^{t_2} B\delta z'(0)dt \\ &= -\int_{t_1}^{t_2} C\delta z(l)dt - \int_{t_1}^{t_2} D\delta z'(l)dt \end{aligned} \tag{4}$$

In this equation, defining four parameters: $A = \rho\ddot{y}(x,t) + EIy^{(4)}(x,t)$, $B = I\ddot{u}'(0,t) - EIu''(0,t) - \tau(t)$, $C = m\ddot{y}(L,t) - EIy^{(3)}(L,t) - F$, $D = EIy''(L,t)$. According to equation (3), the following equation is obtained:

$$-\int_{t_1}^{t_2}\int_0^l A\delta z(x)dxdt - \int_{t_1}^{t_2} B\delta z'(0)dt - \int_{t_1}^{t_2} C\delta z(l)dt - \int_{t_1}^{t_2} D\delta z'(l)dt = 0 \tag{5}$$

Since $\delta z(x)$, $\delta z'(0)$, $\delta z(l)$ and $\delta z'(l)$ are independent variables, that is, all items in the above formula are linearly independent, then $A = B = C = D = 0$ in the formula, thus obtaining the dynamic model:

$$\rho\ddot{z}(x) = -EIz^{(4)}(x) \tag{6}$$

$$\tau = I\ddot{z}'(0) - EIz''(0) \tag{7}$$

$$M = m\ddot{z}(l) - EIz^{(3)}(l) \tag{8}$$

$$z''(l) = 0 \tag{9}$$

Where $\ddot{z}(x) = x\ddot{\theta} + \ddot{y}(x)$, $\ddot{z}(l) = l\ddot{\theta} + \ddot{y}(l)$.

3. Control law design and stability analysis

Through the analysis of the above dynamic models, it is found that the flexible manipulator model has many uncertain parameters and equation orders, which makes the control and vibration suppression of the flexible manipulator more difficult. In this paper, an improved adaptive boundary control method based on the RBF neural network is proposed to realize the control and vibration suppression of flexible manipulators. Meanwhile, the stability of the system is analyzed by the first Lyapunov method.

3.1 Design of neural networks

According to references [5] and [6], an improved RBF neural network is proposed to estimate the unknown disturbance of the system, and the Gaussian function of RBF neural network is expressed as follows:

$$\sigma_i = \frac{2b_i^2}{1+e^{-2V_i\hat{\hat{X}}_i}} - 1 \tag{10}$$

Where $V_i = [v_1,\ v_2,\ \dots ,\ v_n]^T$ is the input vector of the neural network, n indicates the number of input layers in the network, $\sigma_i = [\sigma_1,\ \sigma_2,\ \dots ,\ \sigma_n]^T$ is the output vector of the Gaussian function of the neural network, p is defined as the number of hidden layers of the neural network, $\hat{\hat{X}}_i , b_i$ and σ_i represents vectors in the world coordinate system, the width of the Gaussian basis function of the i th neuron in the hidden layer, the width of the network, and the network of output Gaussian functions. Defining the weight of the neural network as W , the output of the RBF network is $\hat{Y}_{ip} = W^T\sigma$. The structure of this neural network is shown in Figure 2.

3.2 Design of adaptive boundary control law

The flexible manipulator system moves in a wide range, the motion and vibration of flexible manipulator are coupled and influence each other, which interferes with the precise positioning of manipulator to a great extent. Therefore, how to reduce the vibration during the movement of flexible manipulator is an urgent problem to be solved.

The vibration of manipulator can be adjusted by using boundary control method, that is, the control at end boundary of manipulator. To realize the requirements of $y(x,t) \to 0$ and $\dot{y}(x,t) \to 0$, the boundary control input is added to end, and adaptive boundary control law is designed to control end boundary of manipulator to adjust the vibration of manipulator by designing the Lyapunov function.

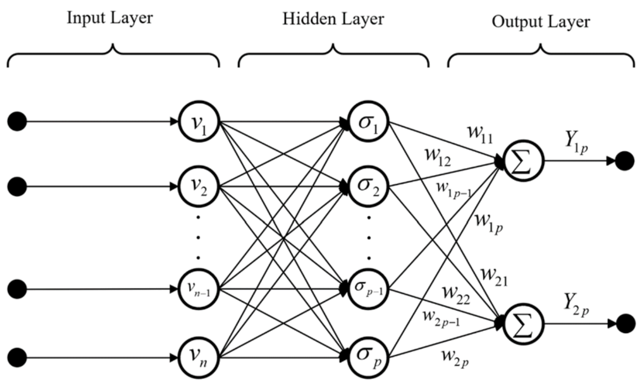

Fig. 2. Neural network structure diagram

For the partial differential equation model, equations (5) to (8), to realize angular response and suppress the vibration of manipulator, the following control law is designed:

$$\tau = -K_p e - K_d \dot{e} \tag{11}$$

$$R = -Ku_a + mz^{(3)}(l) \tag{12}$$

Where K_p, K_d are control gains, $u_a = \dot{z}(l) - z^{(3)}(l)$. According to the actual characteristics of manipulator, $\dot{z}(l)$ and $z^{(3)}(l)$ are both bounded functions, the auxiliary function u_a constructed is also a bounded function. Error $e = \theta - \theta_d$, θ_d is ideal angle, $\dot{e} = \dot{\theta} - \dot{\theta}_d$. R is control accuracy. K is the control gain. The input quantity is adjusted by the control gain, so that the difference calculation is carried out with the actual, and the error is obtained. According to equations (11) and (12), parameter uncertainty has an important impact on the auxiliary function, which directly affects the accuracy. Therefore, the uncertainty error is approximated and eliminated by RBF neural network.

3.3 Proof of system stability

Reference [14] adopted Lyapunov's first method to construct Lyapunov function to prove the stability of system. Equations (10) and (11) are the boundary control laws of the whole system, and the whole system is a closed-loop system. It can be considered that at any point x on the flexible manipulator, as time tends to infinity, there is an actual angle tending to an ideal angle, and the angular velocity is 0, the deformation and velocity in the y direction both tend to 0.

The Lyapunov function is designed as:

$$L(t) = L_1 + L_2 + L_3 + L_4 \tag{13}$$

Where:

$$L_1 = \frac{1}{2}\int_0^l \rho \dot{z}^2(x)dx + \frac{1}{2}EI\int_0^l y''^2(x)dx \tag{14}$$

$$L_2 = \frac{1}{2}I\dot{e}^2 + \frac{1}{2}K_p e^2 + \frac{1}{2}mu_a^2 \tag{15}$$

$$L_3 = \alpha\rho\int_0^l x\dot{z}(x)ze'(x)dx + \alpha I e\dot{e} \tag{16}$$

$$L_4 = \frac{1}{2}(W^T W + V^T V) \tag{17}$$

In above expressions, L_1 is sum of total kinetic energy and total potential energy of flexible manipulator system, L_2 indicates error indicator of the entire system control, L_3 and L_4 is auxiliary items. α is a small positive real number greater than 0.

Let $0 < \alpha_1 < 1$, then define $\alpha \in \left[0, \frac{1}{\alpha_1}\right]$, $\alpha_2 = 1 - \alpha_1$, $\alpha_3 = 1 + \alpha_1$, $0 < \alpha_2 < 1$, $1 < \alpha_3 < 2$. Then exist:

$$0 \le \alpha_2(L_1 + L_2) \le L_1 + L_2 + L_3 \le \alpha_3(L_1 + L_2) \tag{18}$$

For the whole flexible manipulator system, the mass per unit length ρ, bending stiffness EI, moment of inertia I, gain coefficient K and mass m of the control system are all positive real numbers. And the integral in range $x \in [0, l]$ is also greater than 0. In L_4, $W^T W + V^T V \ge 0$, therefore $L(t) \ge 0$, the function $L(t)$ is positive definite.

Differentiating the whole function, we can get following formula:

$$\dot{L}(t) = \dot{L}_1 + \dot{L}_2 + \dot{L}_3 + \dot{L}_4 \tag{19}$$

Overall analysis of the first three items, we can get following item:

$$\begin{aligned}\dot{L}_1 + \dot{L}_2 + \dot{L}_3 \le & -\left(\frac{3}{2}\alpha - 2\alpha l^2 - \frac{2\alpha l^3}{EI}\right)\int_0^l EI(z''(x))^2 dx - \frac{1}{2}\alpha\int_0^l \rho\dot{z}^2(x)dx \\ & -(K_d - \alpha I - K_d\alpha)\dot{e}^2 - (aK_p - K_d\alpha - 2\alpha EIl - 2\alpha l^2)e^2 \\ & -Ku_a^2 + \frac{1}{2}\alpha\rho l\dot{z}^2(l) - (EI - \alpha EIl)(z^{(3)}(x))^2\end{aligned} \tag{20}$$

By selecting α , $EI-\alpha EIl>\frac{1}{2}\alpha\rho l$ holds and guarantees:

$$\frac{1}{2}\alpha\rho l\dot{z}^2(l)-(EI-\alpha EIl)(z^{(3)}(l))^2\le\eta_0(\dot{z}(l)-z^{(3)}(l))^2=\eta_0u_a^2 \tag{21}$$

Where $\eta_0>\max\left(\eta_1,\frac{\eta_1\eta_2}{\eta_1-\eta_2}\right)$, $\eta_1=\frac{1}{2}\alpha\rho l$, $\eta_2=EI-\alpha EIl$.

According to the above two formulas:

$$\dot{L}_1+\dot{L}_2+\dot{L}_3\le-\eta_0(L_1+L_2)\le-\eta_0\frac{L_1+L_2+L_3}{\alpha_3}=-\eta_1(L_1+L_2+L_3) \tag{22}$$

For L_4 , $(\dot{W}^TW+\dot{V}^TV)<0$. In summary, it can be seen that $\dot{L}(t)\le0$, so $\dot{L}(t)$ is negative definite, and since $L(t)\ge0$, the whole system is asymptotically stable.

4. Simulation results and analysis

4.1 Simulated condition

For the flexible manipulator model established above and the designed control law, the vibration suppression is verified by three sets of comparative Simulation. In this paper, using MATLAB/Simulink to establish a controller to verify the feasibility of the algorithm.

Due to the poor rigidity of flexible manipulator, it is easy to generate vibration during operation and is also very vulnerable to interference from the outside world. In the simulation, three types of external interference are simulated to verify the proposed control algorithm. Due to the uncertainty of external interference, it is impossible to simulate completely. Therefore, to better observe, a longer simulation time is selected for simulation. The simulation time is selected as 90s, reference [15], and the residual vibration of motor is reduced, which can also achieve the effect of vibration suppression on flexible manipulator. The commonly used indicators to measure vibration are the displacement, speed, acceleration, angular velocity and so on. In this paper, angular velocity of the motor and the manipulator is selected to measure the effect of vibration suppression. To build a better controller for simulation, the equation of flexible manipulator is now rewritten as a state-space expression:

$$\begin{cases} \dot{x}_1 = x_2 \\ \dot{x}_2 = -\frac{1}{I}[m_l x_2 + k(x_1 - x_3)] \\ \dot{x}_3 = x_4 \\ \dot{x}_4 = -\frac{1}{I}[m_m x_4 - k(x_1 - x_3) - u] \end{cases} \quad (23)$$

Where x_1, x_2, x_3 and x_4 are angle and angular velocity of manipulator, and the angle and angular velocity of motor, respectively. The moment of inertia of both flexible manipulator and motor is 0.04 $N\Box m$, k is stiffness coefficient of 0.8. The structure diagram of designed controller is shown in Figure 3, where $u = K_{P1}x_1 + K_{D1}x_2 + K_{P2}x_3 + K_{D2}x_4$, K_{P1}, K_{D1}, K_{P2}, K_{D2} are the gains of each item, and 1, 0.02, 10, 0.01 are taken respectively. C is identity matrix.

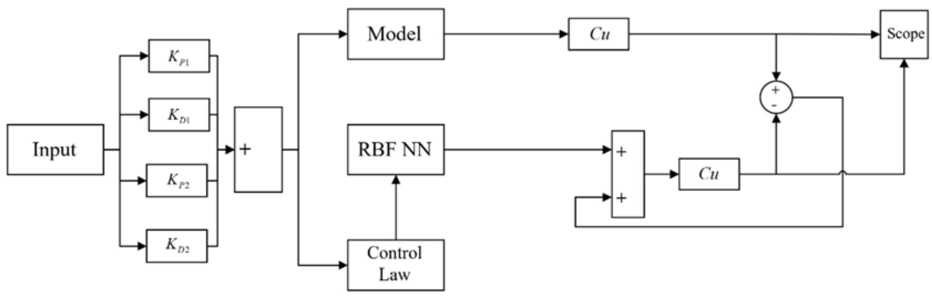

Fig. 3. Structure diagram of the controller

4.2 Analysis of experimental results

In this paper, three kinds of vibration interference input are selected to observe the algorithm and design the vibration suppression of controller. This includes the simplest harmonic vibration, high frequency superimposed vibration, high frequency and high amplitude superimposed vibration to simulate. First select interference as $f_1 = 0.05\sin(t)$. The amplitude is 0.05mm. The results of simulation are shown in Figures 4 and 5. Angle tracking and angular velocity tracking images of flexible manipulator and motor. The motor angle and angular velocity are similar to angular velocity and angular tracking diagram of flexible manipulator. When vibration suppression is not applied to system, there will be a short-term instantaneous change in initial stage of start-up. Angle and angular velocity will have an extremely short-term abrupt increase. After vibration suppression of the model, the instantaneous abrupt change of angle and angular velocity can be eliminated. There are small fluctuations in both flexible manipulator and motor, and these small fluctuations in system can be eliminated by applying suppression, this makes system asymptotically stable.

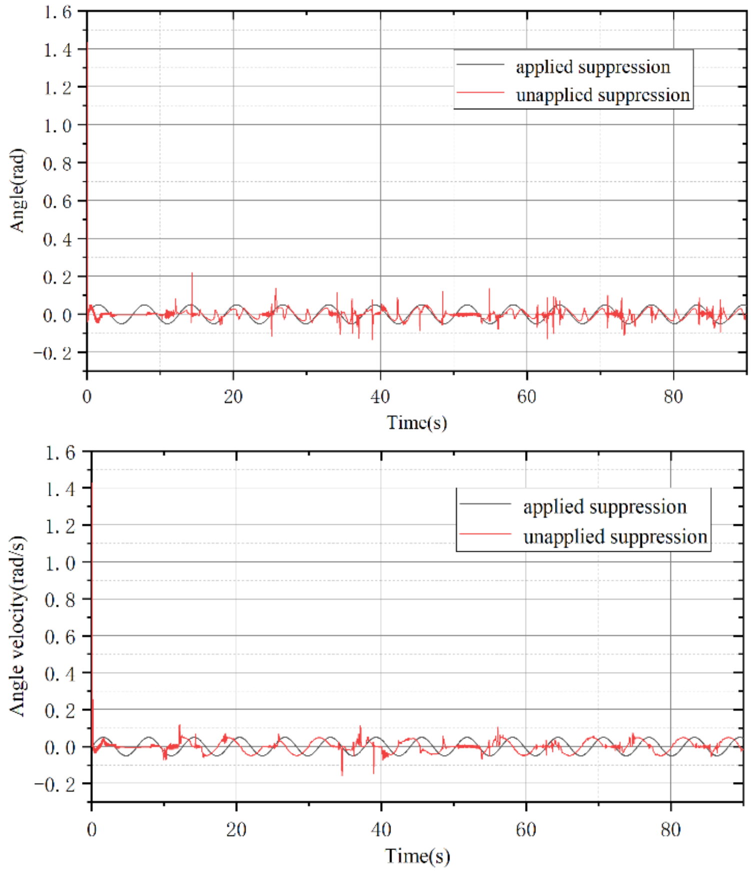

Fig. 4. Angle and angular velocity tracking of flexible manipulator

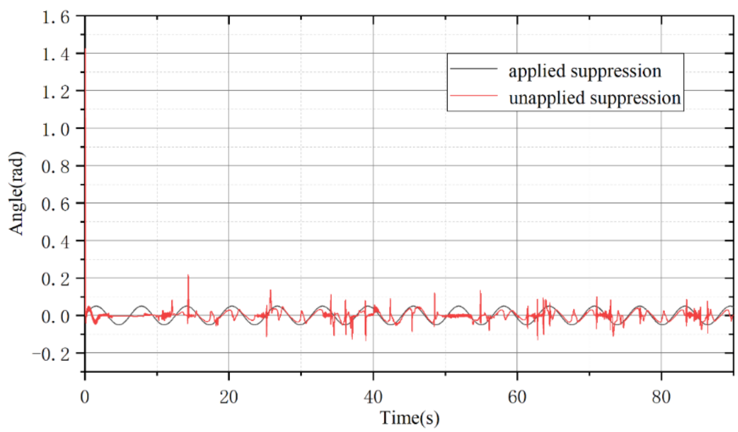

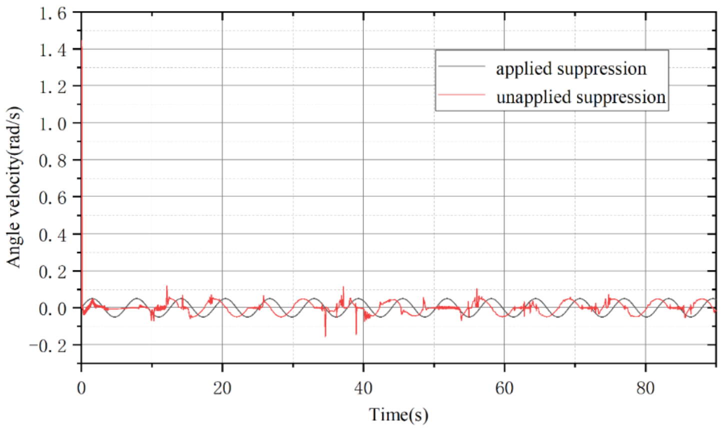

Fig. 5. Motor angle and angular velocity tracking

The second set of experiments add a term with a smaller amplitude but a higher frequency for comparison. Therefore, when selecting the interference of $f_2 = 0.05\sin(t) + 0.03\sin(3t)$. The maximum amplitude is 0.08mm. As shown in Figures 6 and 7, the curve of the unsuppressed vibration is more small amplitude, high frequency vibration, and these high frequency amplitudes can be reduced after the vibration is suppressed. The amplitude of the angular velocity increases significantly when the vibration is not suppressed, and the frequency is higher when the amplitude is higher. After vibration suppression, these high-frequency high-amplitude vibrations can be significantly suppressed.

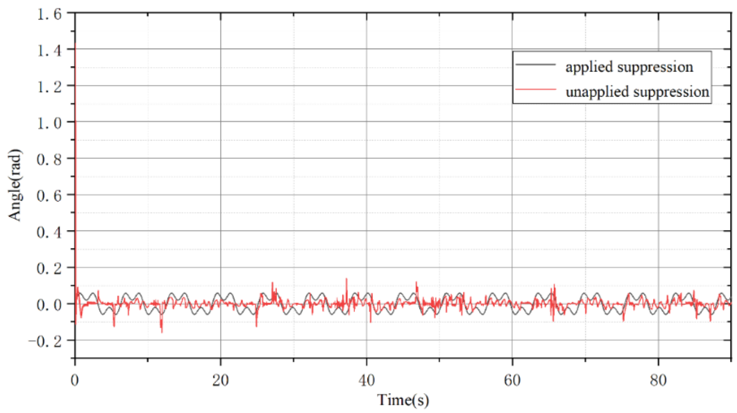

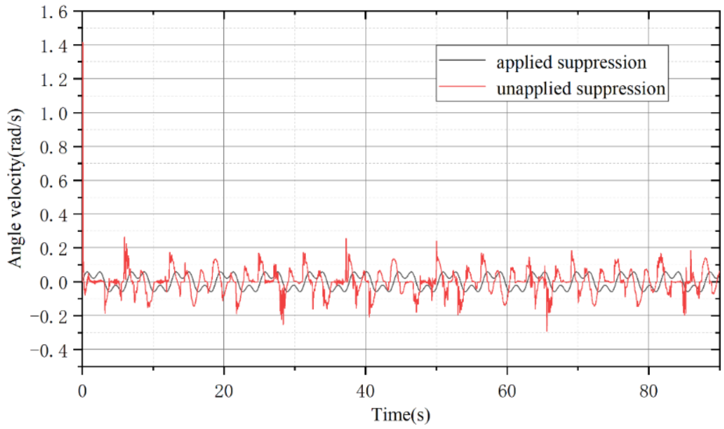

Fig. 6. Angle and angular velocity tracking curve of flexible manipulator

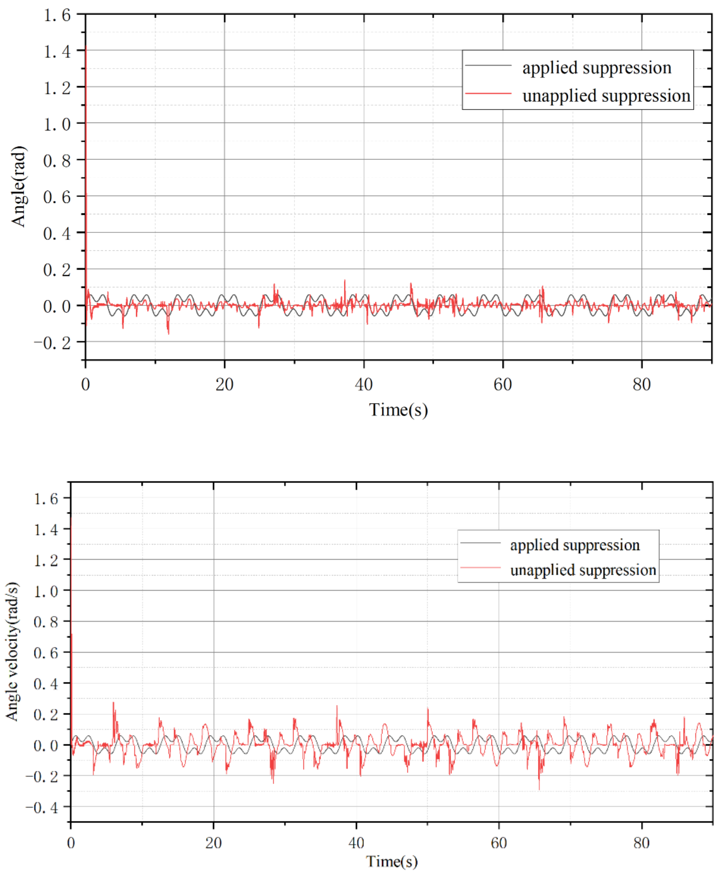

Fig. 7. Motor angle, angular speed tracking

After comparing the two groups above, a disturbance term with the same amplitude as the first group and a further increase in frequency is added for further experimental simulation. $f_3 = 0.05\sin(t) + 0.03\sin(3t) + 0.05\sin(4t)$ is selected. The maximum amplitude is 0.13mm. This is shown in figures 8 and 9, it can be seen from the results that when no inhibition is applied, the frequency and amplitude of angle tracking are further enhanced. During angular velocity tracking, the amplitude increases obviously and the frequency at high amplitude increases further. After the suppression is applied, the amplitude and frequency of the angular velocity fluctuation can be significantly reduced.

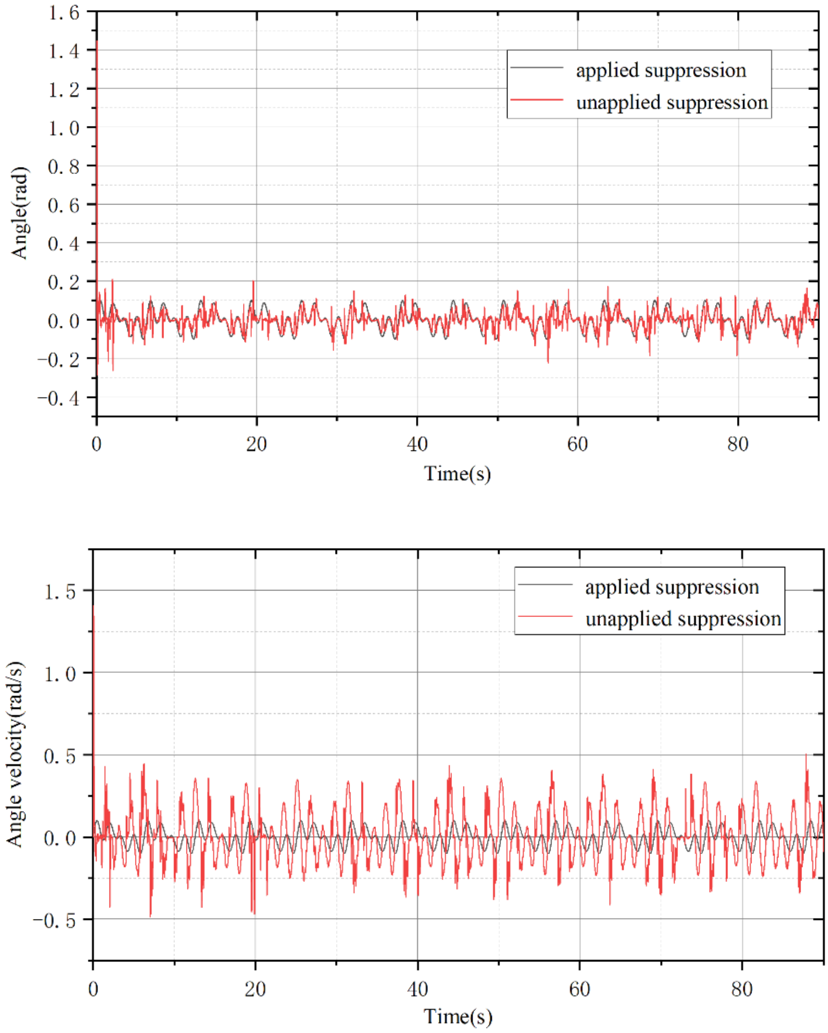

Fig. 8. Angle and angular velocity tracking of the manipulator

Through the above simulation experiment and comparison, when the interference item is a single low frequency, the control algorithm does not suppress the amplitude obviously, but can effectively suppress the high-frequency vibration with small amplitude. With the increase of high-frequency interference, the amplitude of angular fluctuation is not obvious, while the amplitude and frequency of angular velocity fluctuation increase significantly with the increase of frequency, and the frequency also increases when the amplitude of fluctuation is large. In this case, the control algorithm can effectively suppress the angular velocity fluctuation amplitude and high-frequency vibration when multiple disturbances are superimposed.

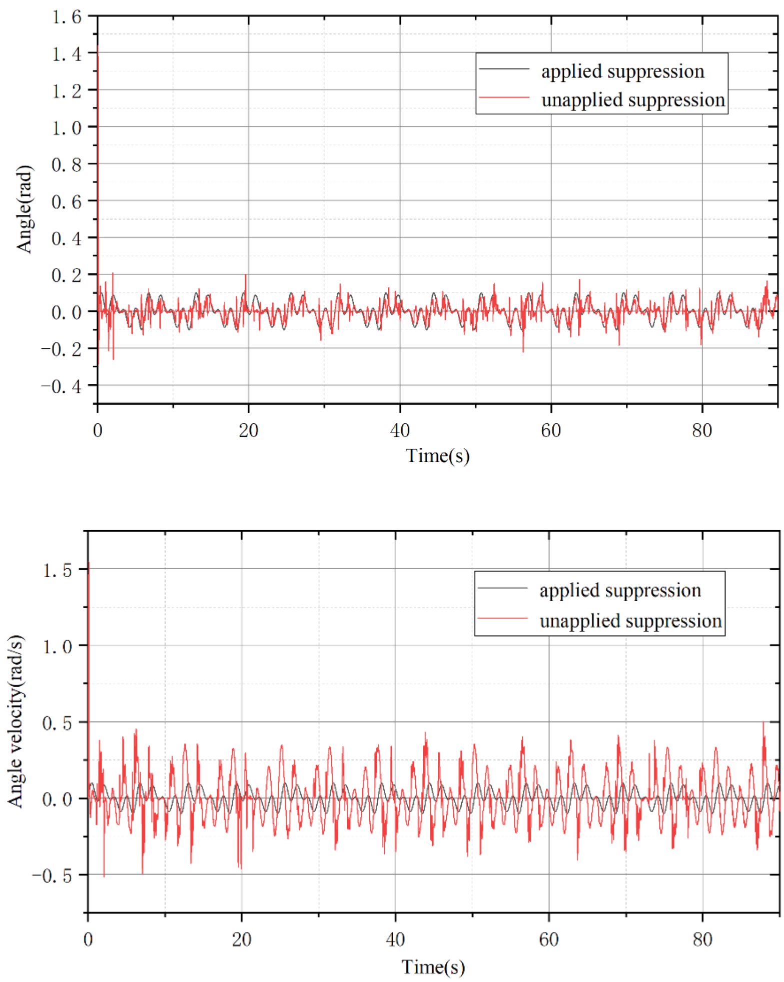

Fig. 9. Motor angle, angular speed tracking

5. Conclusion

In this paper, a flexible manipulator in plane is studied. Firstly, the dynamic model is established. An improved RBF neural network is proposed as an error compensation and adaptive boundary control law to control the flexible manipulator, and the stability of the system is proved by the first Lyapunov method. Finally, the controller was redesigned, and a simulation platform to simulate the interference and amplitudes superimposed. The results show that this control method can effectively suppress the small vibration frequency at low frequency, the angular fluctuation frequency and the high frequency and high amplitude vibration of the angular velocity after the superposition of multiple reactivation modes. It also can effectively suppress the instantaneous vibration fluctuation error of the manipulator starting and can be effective in the operation of the manipulator. Moreover, the angular vibration amplitude and angular velocity vibration amplitude during the operation of the manipulator can be reduced to 0.02rad and 0.02rad/s.

In future research, the finite element method can be used to further analyze the mode of the whole flexible manipulator system. This paper only considers the linear model. Therefore, the nonlinear state-space equation can be established for simulation, to further improve the authenticity and accuracy of the simulation.

Acknowledge

This work was supported by the National Natural Science Foundation of China (62073239).

REFERENCES

[1]. *J. Kim, M. Uchiyama*. "Vibration mechanism of constrained spatial flexible manipulators". JSME International Journal Series C-Mechanical Systems Machine Elements and Manufacturing, **vol**. 41, no. 1, Mar. 2003, pp. 123-128.

[2]. *Z. Mohamed, M. Tokhi*. "Hybrid control schemes for input tracking and vibration suppression of a flexible manipulator". Proceedings of the Institution of Mechanical Engineers Part I-Journal of Systems and Control Engineering. **vol**. 217, no. 1, Jan. 2003, pp. 23-34.

[3]. *V. Phan, N. Goo, H. Park*. "Vibration suppression of a flexible robot manipulator with a lightweight piezo-composite actuator". International Journal of Control Automation and Systems. **vol**. 7, no. 2, Apr 2009, pp. 243-251.

[4]. *M. Shaheed, M, Tokhi*. "Modelling and open-loop control of a single-link flexible manipulator with neural networks". Journal of Low Frequency Noise Vibration and Active Control. **vol**. 20, no. 2, Jan 2001, pp.105-131.

[5]. *J. Liu, L. Li.* "Neural-network-based adaptive fault-tolerant vibration control of single-link flexible manipulator". Transactions of the Institute of Measurement and Control, **vol.** 42, no. 3, Feb. 2020, pp. 430-438.

[6]. *C. He, F. Zhang, J. Jiang*. “Adaptive boundary control of flexible manipulators with parameter uncertainty based on RBF neural network”. Shock and Vibration, **vol. 2020**, Nov. 2020, pp. 1-13.
[7]. *W. He, H. Gao, C. Zhou, et al*. “Reinforcement learning control of a flexible two-link manipulator: an experimental investigation”. IEEE Transactions on Systems, Man, and Cybernetics: Systems, **vol**. 51, no. 12, Dec. 2021, pp. 7326-7336.
[8]. *Y. Li, S. Ge, Q. Wei, et al*. “An online trajectory planning method of a flexible-link manipulator aiming at vibration suppression”. IEEE Access, **vol**. 8, Jan 2020, pp. 13616-130632.
[9]. *P. Zhao, Y. Zhou*. “Active vibration control of flexible-joint manipulators using accelerometers”. Industrial Robot-The Interna Journal of Robotics Research and Application, **vol**. 47, no. 1, Jan 2020, pp. 33-44.
[10]. *S. Jia, J. Shan*. “Velocity-free trajectory tracking and active vibration control of flexible space manipulator”. IEEE Transactions Aerospace and Electronic Systems, **vol**. 58, no.1, Feb 2022, pp. 435-450.
[11]. *W. He, F. Kang, L. Kong, et al*. “Vibration control of a constrained two-link flexible robotic manipulator with fixed-time convergence”. IEEE Transactions on Cybernetic, **vol**. 52, no. 7, Jul 2022, pp. 5973-5983.
[12]. *W. He, S. Ge, B. How, et al*. “Robust adaptive boundary control of a flexible marine riser with vessel dynamics”. Automatica, **vol**. 47, no.4, Apr 2011, pp. 722-732.
[13]. *L. Zhang, J. Liu*, “Adaptive boundary control for two-link manipulator based on partial differential equations dynamic model”, IET Control Theory & Application, **vol**. 7, no. 1, Jan 2013, pp. 41-53.
[14]. *T. Jiang, J. Liu*, *W. He*. “Boundary control for a flexible manipulator based on infinite dimensional disturbance observer”, Journal of Sound and Vibration, **vol**. 348, no. 21, Jul 2015, pp. 1-14.
[15]. *Y. Yang, Y. Wei, J. Lou, et al*. “Dynamic modeling and adaptive vibration suppression of a high-speed macro-micro manipulator”, Journal of Sound and Vibration, **vol**. 422, May 2018, pp. 318-342.